



HAL
open science

Three-dimensional muscle loss assessment: a novel computed tomography–based quantitative method to evaluate rotator cuff muscle fatty infiltration

Jean-David Werthel, François Boux de Casson, Gilles Walch, Pascal Gaudin, Philipp Moroder, Joaquin Sanchez-Sotelo, Jean Chaoui, Valérie Burdin

► To cite this version:

Jean-David Werthel, François Boux de Casson, Gilles Walch, Pascal Gaudin, Philipp Moroder, et al.. Three-dimensional muscle loss assessment: a novel computed tomography–based quantitative method to evaluate rotator cuff muscle fatty infiltration. *Journal of Shoulder and Elbow Surgery*, 2022, 31 (1), pp.165-174. 10.1016/j.jse.2021.07.029 . hal-03384412

HAL Id: hal-03384412

<https://imt-atlantique.hal.science/hal-03384412>

Submitted on 5 Jan 2024

HAL is a multi-disciplinary open access archive for the deposit and dissemination of scientific research documents, whether they are published or not. The documents may come from teaching and research institutions in France or abroad, or from public or private research centers.

L'archive ouverte pluridisciplinaire **HAL**, est destinée au dépôt et à la diffusion de documents scientifiques de niveau recherche, publiés ou non, émanant des établissements d'enseignement et de recherche français ou étrangers, des laboratoires publics ou privés.



Distributed under a Creative Commons Attribution - NonCommercial 4.0 International License

**3D Muscle Loss (3DML) assessment: A novel CT-based quantitative method
to evaluate rotator cuff muscle fatty infiltration**

Short running title: Quantitative 3D Muscle Loss Assessment

Jean-David Werthel, MD, MS^{1,2*}

François Boux de Casson, PhD³

Gilles Walch, MD^{4,5}

Pascal Gaudin, MD⁶

Philipp Moroder, MD⁷

Joaquin Sanchez-Sotelo, MD⁸

Jean Chaoui, PhD⁹

Valérie Burdin, PhD²

¹Hôpital Ambroise Paré, 9 avenue Charles de Gaulle, 92100 Boulogne-Billancourt, France

²IMT Atlantique, LaTIM INSERM U1101, Brest, France

³Tornier, 38330 Montbonnot, France

⁴Centre Orthopédique Santy, 24 Avenue Paul Santy 69008, Lyon, France.

⁵Ramsay Générale de Santé, Hôpital Privé Jean Mermoz, Lyon, France.

⁶Clinique Jouvenet, 6, square Jouvenet, 75016, Paris, France

⁷Charité – Universitätsmedizin Berlin, Berlin, Germany

⁸Mayo Clinic, Rochester, MN, USA

⁹Imascap, 29280 Plouzané, France

*Corresponding author and requests for reprints authors

Jean-David Werthel, MD, MS

Hôpital Ambroise Paré

9 avenue Charles de Gaulle

92100 Boulogne-Billancourt, France

Disclaimers:

Funding: No funding was disclosed by the author(s).

Conflicts of interest: Dr Werthel receives royalties for shoulder prosthesis design from FH Orthopedics. Dr Boux de Casson is an employee of Wright Medical. Dr Walch receives royalties for shoulder prosthesis design from Wright Medical. Dr Moroder receives royalties from Arthrex Inc. and NCS Lab for shoulder related products. Dr Sanchez-Sotelo receives royalties for shoulder prosthesis design from Wright Medical-Stryker. Prof Chaoui owns stocks and stock options from Wright Medical. The other authors, their immediate families, and any research foundation with which they are affiliated did not receive any financial payment or other benefits from any commercial entity related to the subject of this article.

This study was approved by the Institutional Review Board of the Ethical Committee of Hôpital Privé Jean Mermoz, Lyon, France (COS-RGDS-2020-05-001-WALCH-G).

1 **Abstract**

2

3 ***Introduction***

4

5 Rotator cuff fatty infiltration (FI) is one of the most important parameters to predict the
6 outcome of certain shoulder conditions. The primary objective of this study was to define a
7 new computed tomography (CT)-based quantitative 3-dimensional (3D) measure of muscle
8 loss (3DML) based on the rationale of the 2-dimensional (2D) qualitative Goutallier score.
9 The secondary objective of this study was to compare this new measurement method to
10 traditional 2D qualitative assessment of FI according to Goutallier et al and to a 3D
11 quantitative measurement of fatty infiltration (3DFI).

12

13 ***Materials and Methods***

14

15 102 CT scans from healthy shoulders (46) and shoulders with cuff tear arthropathy (21),
16 irreparable rotator cuff tears (18), and primary osteoarthritis (17) were analyzed by three
17 experienced shoulder surgeons for subjective grading of fatty infiltration according to
18 Goutallier and their rotator cuff muscles were manually segmented. Quantitative 3D
19 measurements of fatty infiltration (3DFI) were completed. The volume of muscle fibers
20 without intra-muscular fat was then calculated for each rotator cuff muscle and normalized to
21 the patient's scapular volume to account for the effect of body size (NV_{fibers}). Three-
22 dimensional muscle mass (3DMM) was calculated by dividing the NV_{fibers} value of a given
23 muscle by the mean expected volume in healthy shoulders. Three-dimensional muscle loss
24 (3DML) was defined as $1-(3DMM)$. The correlation between Goutallier grading, 3DFI, and
25 3DML was compared using a Spearman Rank correlation.

26

27 ***Results***

28 Interobserver reliability for the traditional 2D Goutallier grading was moderate for the
29 infraspinatus (ISP=0.42) and fair for the supraspinatus (SSP=0.38),
30 subscapularis (SSC=0.27) and teres minor (TM=0.27). 2D Goutallier grading was found to be
31 significantly and highly correlated with 3DFI (SSP=0.79, ISP=0.83, SSC=0.69,
32 TM=0.45) and 3DML (SSP=0.87, ISP=0.85, SSC=0.69, TM=0.46) for all four rotator cuff
33 muscles ($p<0.0001$). This correlation was significantly higher for 3DML than for the 3DFI for
34 the SSP only ($p=0.01$).

35 The mean values of 3DFI and 3DML were 0.9% and 5.3% for Goutallier-0, 2.9% and 25.6%
36 for Goutallier-1, 11.4% and 49.5% for Goutallier-2, 20.7% and 59.7% for Goutallier-3, and
37 29.3% and 70.2% for Goutallier-4, respectively.

38

39 **Conclusion**

40 The Goutallier score has been helping surgeons by using 2-dimensional CT-scan slices.
41 However, this grading is associated with suboptimal interobserver agreement. The new
42 measures we propose provide a more consistent assessment that correlates well with
43 Goutallier's principles. As 3DML measurements incorporate atrophy and fatty infiltration,
44 they could become a very reliable index for assessing shoulder muscle function. Future
45 algorithms capable of automatically calculating the 3DML of the cuff could help in the
46 decision process for cuff repair and the choice of anatomic or reverse shoulder arthroplasty.

47

48 Level of Evidence: Anatomy Study; Imaging

49 Keywords: Goutallier; 3D Goutallier; muscle volume; 3D CT scan; atrophy; volumetric
50 analysis

51

52

53

54 Rotator cuff fatty infiltration (FI) is recognized as one of the most important parameters to
55 predict the outcome the outcome of certain shoulder procedures^{5; 8; 9; 11; 23; 33} and it is
56 considered crucial for clinical decision-making prior to rotator cuff repair and shoulder
57 arthroplasty^{14; 20; 43}. Goutallier et al⁹ first reported a method to subjectively and qualitatively
58 stage intra-muscular fatty infiltration into 5 grades using computed tomography (CT) on axial
59 views. This method was then adapted by Fuchs et al for its application on magnetic resonance
60 imaging (MRI) on T1-weighted sequences⁵. These two qualitative 2-dimensional (2D)
61 classifications are known to have poor intra- and inter-observer reliability between 0.26 and
62 0.81 for intra-observer reliability and between 0.36 and 0.6 for inter-observer reliability.^{30; 35;}
63 ⁴¹, and several recent studies have shown how modern imaging sequences and techniques
64 have the potential to provide a better estimate of FI by allowing accurate quantitative
65 calculation of the intra-muscular fat fraction after manual segmentation of rotator cuff muscle
66 boundaries either on 2D sagittal Y-views^{17; 22; 28; 29; 31} or in 3 dimensional (3D) images^{16; 26; 28;}
67 ⁴¹. A number of imaging techniques (single-voxel MR spectroscopy³¹, spectroscopic gradient
68 echo imaging¹⁷, two-point Dixon imaging^{16; 26; 29} or chemical shift-based water-fat separation

69 techniques^{22; 28}) have been reported to correlate with Goutallier scores. However, the
70 objective quantitative percentage of intramuscular fat calculated with these methods was
71 much lower than the expected fat ratio as determined qualitatively according to Goutallier^{28;}
72 ⁴¹. This is probably due to two reasons: first, distribution of intra-muscular fat is not uniform
73 inside the muscle body^{15 2; 18; 27; 28} and as such 2-dimensional assessments cannot capture 3-
74 dimensional FI measurements ^{19; 41}; and secondly, the subjective qualitative assessment of the
75 Goutallier score may sometimes be difficult to apply, since the precise distinction between
76 atrophy and fatty infiltration is often unclear in the literature as it is often difficult to
77 distinguish the boundaries between intra- and extra-muscular fat in cases of severe muscle
78 atrophy and FI (Figure 1).

79 We therefore hypothesized that the qualitative Goutallier score would be better translated
80 quantitatively by calculating the percentage of remaining muscle tissue (independent of intra-
81 or extra-muscular fat) rather than by calculating the percentage of fat within the muscle. The
82 primary objective of this study was to define a new quantitative 3-dimensional (3D) measure
83 of muscular loss (3DML) based on rationale of the 2-dimensional (2D) qualitative Goutallier
84 score. The secondary objective of this study was to compare this new measurement method to
85 the traditional 2D qualitative assessment of FI according to Goutallier et al and to a 3D
86 quantitative measurement of fatty infiltration (3DFI).

87

88

89

90 **Materials and Methods**

91

92 This study was approved by the Institutional Review Board of the Ethical Committee of
93 Hôpital Privé Jean Mermoz, Lyon, France (COS-RGDS-2020-05-001-WALCH-G).

94

95 ***Study Cohort***

96 We retrospectively reviewed shoulder CT-scans performed between 2015 and 2020 and
97 obtained from a database incorporating 4 institutions (Lyon, Nice and Paris, France, Belo
98 Horizonte, MG, Brazil). The CT-scan exams had been performed using one of two CT scan
99 systems (Revolution CT, GE Healthcare, Chicago, IL, USA or Siemens Somatom CT
100 Scanner, Siemens Healthcare, Erlangen, Germany) with the patient positioned supine on the
101 CT table. CT-scan exams of healthy shoulders and shoulders with primary osteoarthritis
102 (OA), cuff tear arthropathy (CTA), and irreparable rotator cuff tears (IRCT) were included

103 provided they had been obtained using the following acquisition parameters: slice thickness
104 <1.2 mm, number of slices > 200, field of view: whole scapula, X-Y resolution <0.5mm,
105 matrix size: 512 x 512, kV140, mA>300, and both bone and soft-tissue algorithms.
106 Our final study sample included a total of 102 CT-scans (healthy shoulders 46, CTA 21,
107 ICRT 18, and OA 17 shoulders). The CT of healthy shoulders had been obtained from
108 patients aged older than 18 years without shoulder pathology or injury in the setting of (1)
109 polytrauma, (2) traumatic head injury, or (3) unilateral shoulder trauma with a contralateral
110 normal shoulder. The CT-scan images of patients with CTA, IRCT or OA were preoperative
111 CT-scans performed prior to shoulder arthroplasty. Shoulders with full-thickness rotator cuff
112 tears were classified as CTA if they were \geq grade 4 in the Hamada classification¹⁰ and as
113 IRCT if they had at least two irreparable rotator cuff tendons but no glenohumeral arthritis
114 (Hamada < 4). Patient's demographics are detailed in Table 1.

115

116 ***Qualitative 2D analysis of FI: traditional Goutallier score using 2D CT images***

117 Axial and sagittal CT slices were analyzed according to the principles underlying the
118 Goutallier et al⁹ and Fuchs et al⁵ protocols for the presence of FI, which was classified
119 according to the 5-grade qualitative scale described by Goutallier et al⁹: Grade 0, normal;
120 Grade 1, some fatty streaks; Grade 2, more muscle than fat; Grade 3, equal amounts of fat and
121 muscle; and Grade 4, more fat than muscle. All the CT-scans were examined independently
122 by 3 different fellowship-trained shoulder surgeons (J.D.W, P.M., P.G.) in order to assess the
123 inter-rater reliability of this subjective quantitative method. The final grading of each muscle
124 used for analysis was based on consensus agreement where 2/3 or 3/3 surgeons had classified
125 the same grade. A difference of more than 1 grade required that all surgeons reviewed the
126 examination together again in order to reach consensus.

127 ***Three-Dimensional Muscle Reconstruction***

128 The soft-tissue DICOM (Digital Imaging and Communications in Medicine) images for each
129 CT scan were manually segmented using the Slicer version 4.10.0 software (Slicer
130 Community Boston, MA, USA; <http://slicer.org>). Muscle boundaries were manually
131 identified and marked to segment the four rotator cuff muscles: supraspinatus, subscapularis,
132 infraspinatus and teres minor. To create a robust process, muscle boundaries were identified

133 on each image slice in all 3 planes (coronal, axial and sagittal). The segmentations were
134 performed either by a shoulder fellowship-trained orthopedic surgeon or by trained
135 technicians; segmentation performed by technicians was verified and corrected when needed
136 by the same orthopedic surgeon that had completed manual segmentation of a proportion of
137 the CT. Published threshold values were used to identify muscle and fat tissue¹. Extra-
138 muscular fat was not assessed. The volume of muscle fibers without intra-muscular fat
139 (V_{fibers}) and the volume of intra-muscular fat (V_{imfat}) were calculated in cm^3 for each muscle.

140 *Quantitative 3D analysis of FI (3DFI), muscle mass (3DMM) and muscle loss (3DML)*

141 Quantitative calculation of FI (3DFI) was possible once the muscle fiber volume (V_{fibers}) and
142 the intra-muscular fat volume (V_{imfat}) have been calculated. The following formula was
143 applied to each rotator cuff muscle:

$$144 \quad 3DFI = \frac{V_{imfat}}{V_{fibers} + V_{imfat}}$$

145 The bone DICOM series were then automatically segmented using a validated 3D-software
146 (BluePrint, v2.1.6, Tornier SAS, France) which provides a 3D model of the scapula and
147 allows automatic calculation its volume in cm^3 . Each measurement of muscle fiber volume
148 was then normalized to the patient's scapular volume to account for the effect of body size on
149 muscle volume²⁴. This allowed us to calculate the normalized volume of muscle fibers
150 (NV_{fibers}) for each rotator cuff muscle. Mean NV_{fibers} were calculated for each muscle in the 4
151 different groups of patients (Healthy Controls, IRCT, CTA, OA). In order to establish a frame
152 of reference for normal muscle volume, the NV_{fibers} value for each muscle was divided by the
153 theoretical volume that this muscle would have if it were healthy. This theoretical volume was
154 determined by calculating the mean NV_{fibers} of the healthy shoulders, which were used to
155 obtain a reference value for males and females for each of the rotator cuff muscles (Ref
156 NV_{fibers}). Table 2 summarizes mean NV_{fibers} for each muscle and each group. Quantitative
157 calculation of three-dimensional muscle mass (3DMM) was completed by dividing the
158 NV_{fibers} value for a given muscle by the Ref NV_{fibers} of that muscle.

$$159 \quad 3DMM = \frac{NV_{fibers}}{Ref\ NV_{fibers}},$$

160 3D muscle loss (3DML) is then determined by subtracting 3DMM from 100.

161

$$3DML = 100 - 3DMM$$

162 For example, the average RefNV_{fibers} value of the infraspinatus for males is 1.4 (Table 1). If
163 the NV_{fibers} infraspinatus measurement of a given shoulder of a male patient is 0.88, the
164 infraspinatus 3DMM for such shoulder would be $0.88/1.40 = 63\%$, which means that 63% of
165 the expected muscle mass is still present and the remaining 37% of the expected muscle mass
166 is been replaced by infiltrated fat ($3DML = 1 - 0.88/1.4 = 37\%$). Two examples can be seen in
167 Figures 2 and 3.

168

169 *Statistical Analysis*

170 Reliability of agreement between the three raters of the Goutallier grade was assessed using a
171 Fleiss kappa (k). Fleiss Kappa value and 95% CI were computed for each muscle, for the
172 whole cohort but also for each diagnostic group (Healthy Controls, CTA, IRCT, OA).
173 Concordance was evaluated using the table of Landis et al²¹.

174

175 One-way analysis of variance was used to test the difference between the means of several
176 diagnostic subgroups (Healthy Controls, CTA, MRCT, OA) of a continuous variable (3DFI or
177 3DML). Levene's test was used to check the equality of variances. The hypothesis that the
178 means of at least two of the subgroups differ significantly is accepted if the P value of the F
179 statistic is less than 0.05. The pairwise comparison of the subgroups was then calculated using
180 the Tukey-Kramer test. If the Levene test is positive ($p < 0.05$), then the variances in the
181 different groups are different and we used a non-parametric statistic. In that case, the Kruskal-
182 Wallis test (H-test) was used. For the whole cohort, but also each diagnostic group (Healthy
183 Controls, CTA, MRCT, OA), the correlation between the consensus Goutallier score and the
184 quantitative 3D analysis of fatty infiltration (3DFI) and 3DML was computed using a
185 Spearman Rank Correlation. The coefficient of rank correlation, rho, was assessed using a
186 Steiger test.

187

188 For all tests, the level of statistical significance was set at $p < 0.05$. Statistical analyses were
189 performed using R (v3.6.1, R Foundation) or MedCal (v19.4.0, MedCalc Software Ltd.)
190 depending on the test.

191

192

193 **Results**

194

195 ***Goutallier inter-observer reliability***

196

197 Analysis of the interobserver reliability showed fair interobserver reliability for supraspinatus,
198 subscapularis and teres minor FI, with k values of 0.38 (range [0.31; 0.44]), 0.27 (range [0.22;
199 0.33] and 0.27 (range [0.19; 0.36] respectively. Interobserver reliability was moderate for
200 infraspinatus FI, with a k value of 0.42 (range [0.35; 0.48]). Inter-observer reliability is
201 detailed in Table 3.

202

203 ***Quantitative 3D analysis of fatty infiltration (3DFI) and muscle loss (3DML)***

204

205 The mean 3DFI and 3DML are detailed for each rotator cuff muscle and for each patient
206 group (Healthy Controls, CTA, MRCT, OA) in Tables 4 and 5.

207

208 The mean 3DFI was significantly greater for all four rotator cuff muscles in pathological
209 groups than in the healthy control group ($p < 0.0001$). Among the pathological groups, the
210 mean FI was significantly higher for the supraspinatus of CTA and MRCT patients than for
211 OA patients ($p < 0.02$) and for the infraspinatus of CTA patients than for OA patients
212 ($p < 0.001$).

213 The mean 3DML was significantly greater for all four rotator cuff muscles in pathological
214 groups than in the healthy control group ($p < 0.0001$). Among the pathological groups, the
215 mean 3DML was significantly higher for the supraspinatus of CTA and MRCT patients than
216 for OA patients ($p < 0.001$) and for the infraspinatus of CTA patients than for OA patients
217 ($p < 0.005$).

218 The correlation between the consensus 2D Goutallier score and the quantitative 3D analysis
219 of FI and ML is detailed in Table 6. For all rotator cuff muscles, mean values of 3DFI were
220 $0.9\% \pm 1.5$ for Goutallier 0 muscles, $2.9\% \pm 4.6$ for Goutallier 1 muscles, $11.4\% \pm 9.9$ for
221 Goutallier 2 muscles, $20.7\% \pm 17.5$ for Goutallier 3 muscles and $29.3\% \pm 23.4$ for Goutallier
222 4 muscles. Mean values of 3DML for all four rotator cuff muscles were $5.3\% \pm 17.4$ for
223 Goutallier 0 muscles, $25.6\% \pm 22.3$ for Goutallier 1 muscles, $49.5\% \pm 16.3$ for Goutallier 2
224 muscles, $59.7\% \pm 13.9$ for Goutallier 3 muscles and $70.2\% \pm 16.3$ for Goutallier

225 4 muscles. Results for each rotator cuff muscle are detailed in Table 6. The 2D Goutallier
226 score was significantly and highly correlated to the volume measurement of 3DFI and 3DML
227 for all four rotator cuff muscles ($p < 0.0001$). This correlation was significantly higher for the
228 3DML than for the measure of 3DFI for supraspinatus ($p = 0.01$).

229

230

231

232 **Discussion**

233

234 Rotator cuff FI is extremely important in the decision-making process prior to rotator cuff
235 repair or shoulder arthroplasty. Despite advances in preoperative planning for shoulder
236 arthroplasty using dedicated software with three-dimensional assessments, currently most
237 surgeons grade rotator cuff FI subjectively on two-dimensional CT or MRI. The results of our
238 study seem to indicate that the interobserver reliability of the Goutallier classification for FI
239 on CT is only fair to moderate, in accordance with prior studies^{30; 34; 41}. In addition, our study
240 seems to indicate that quantitative measurements of muscle mass and muscle loss may be of
241 value when assessing rotator cuff degeneration in shoulders with OA, CTA and IRCT.

242 Several authors have proposed to improve the assessment of FI by using 2-dimensional
243 quantitative methods^{28; 37}. These methods were reported to be significantly correlated with
244 Goutallier grades. However, we believe that analyzing a 3-dimensional structure on a single
245 two-dimensional slice is incorrect and subject to significant bias, particularly considering that
246 fat is not homogeneously distributed inside rotator cuff muscles^{27; 42}. Vidt et al⁴¹ have recently
247 demonstrated that single-image assessments are not able to capture 3D measures of fatty
248 infiltration, and that the use of a 3D quantitative method allows better discrimination between
249 the various Goutallier grades.

250 In our study, when we calculated 3DFI values, we found a very different percentage of fat to
251 muscle ratio than expected according to Goutallier criteria. Indeed, Goutallier grades 3 and 4
252 are traditionally considered to correspond to a muscle replacement by fat of 50% or more, but
253 our mean 3DML values were 20.7% and 29.3% respectively. This finding is in agreement
254 with previous studies^{28; 41} which have also found much lower quantitative values than
255 expected after qualitative assessment. In other words, it only takes loss of 30% of muscle
256 volume to translate into a two-dimensional visual estimate of over 50% fatty infiltration
257 replacement.

258

259 Muscle atrophy and FI have been recognized as independent predictive parameters of
260 outcome for a number of surgical procedures^{5; 8; 9; 11; 23; 33}. However, as independent as these
261 parameters may be, all the methods that we currently use to assess them inevitably make them
262 dependent on each other. Indeed, measures of muscle volume and muscle atrophy (tangent
263 sign⁴⁴, occupation ratio³⁸) typically include intra-muscular fat^{6-8; 25; 39} and, the measures of
264 fatty infiltration depend on muscle volume as they are expressed as the ratio of intra-muscular
265 fat volume to muscle volume^{5; 9}. Therefore, a decrease in muscle volume, with no change in
266 the volume of intra-muscular fat, automatically leads to an increase in the fatty infiltration
267 ratio. It has been shown that increased percentages of fat observed in cases of severe fatty
268 infiltration are more related to muscle atrophy than to increased fat volume⁴¹. Furthermore, it
269 is not clear from the Goutallier score whether fatty infiltration includes only intra-muscular
270 fat or both intra- and extra-muscular fat, especially in cases of severe fatty infiltration and
271 muscle atrophy.

272

273 For these reasons, we reasoned that assessment of rotator cuff muscle degeneration could be
274 much improved by developing quantitative three-dimensional assessments of remaining
275 muscle mass and muscle loss. The method presented in our study is complex and tedious,
276 since it requires manual segmentation and two normalization steps. However, they provided
277 the basis and ground truth for training algorithms that in the near future will incorporate
278 automatic muscle segmentation using statistical models and deep learning techniques^{3; 32}.
279 Furthermore, a major benefit of the proposed 3DML measurement is that it integrates both
280 atrophy and fatty infiltration into a single value, which will hopefully best correlate with
281 remaining strength as well as predicted outcomes after surgery^{12; 13; 40}.

282 Interestingly, although the Goutallier score was found to be relatively unreliable when
283 evaluated by a single shoulder-specialized surgeon, this was no longer the case when a
284 consensus Goutallier score was determined among 3 surgeons. Indeed, the consensus values
285 were strongly and significantly correlated with both 3DFI and 3DML measurements, with
286 superior correlation with the 3DML measurements for the supraspinatus muscle (Table 6). In
287 addition, 3DML values were found to be much closer to the expected Goutallier fat ratio than
288 3DFI values. Indeed, the mean 3DML values were found to be 5.3% for Goutallier-0 muscles,
289 25.6% for Goutallier-1, 49.5% for Goutallier-2, 59.7% for Goutallier-3 and 70.2% for
290 Goutallier-4, suggesting that 3DML values correspond better to the traditional Goutallier
291 grading currently used in practice. We suspect that calculation of 3DML values will be the
292 most useful FI parameter to consider when assessment of muscle atrophy and FI is fully

293 automated.

294 Our study has several limitations. Firstly, the size of the cohort of pathological shoulders was
295 relatively small; this was due to difficulties obtaining CT scans with both bone and soft tissue
296 algorithms and the entire scapula, which was unfortunately often truncated at its medial or
297 distal tip. With the recent trend to use high quality CT protocols in preoperative planning
298 software, it is likely that future CT scans will routinely include the entire scapula. Secondly,
299 we did not perform inter- and intra- observer reliability analysis for manual segmentation
300 because of the high number of cases and the extensive amount of time needed to segment the
301 entire rotator cuff. Thirdly, most studies analyzing muscle volume have been based on MR-
302 imaging, using techniques that generate more accurate quantitative fat-fraction maps which
303 distinguish fat and muscle from other tissues such as vessels ; however, we chose to
304 investigate CT-imaging with a soft-tissue algorithm for four main reasons: (1) MRI and CT
305 have been shown to be equally effective in assessing supraspinatus atrophy³⁶ and in
306 measuring rotator cuff cross-sectional area; (2) CT-imaging allowed us to automatically
307 segment the scapula using a validated 3D-software (BluePrint, v2.1.6, Tornier, France) and
308 calculate the volume of the scapula in cm³; (3) the proportion of pixels not clearly attributable
309 to muscle or fat was neglectable compared to the number of pixels which are clearly
310 identifiable as muscle or fat, (4) it is easy to obtain CT-scans including the whole scapula
311 with enough slices to perform multiplanar and 3D reconstructions, while this is more
312 challenging to obtain on MRI; and (5) CT is widely available, fast and routinely used in
313 preoperative planning for shoulder arthroplasty⁴, where adding soft tissue algorithms to bone
314 algorithms is simple, fast and relatively inexpensive. At present time, the method described in
315 our study is not intended to be incorporated into routine surgical practices until automation of
316 this process will easily allow us to accurately and objectively determine rotator cuff muscle
317 mass and muscle loss.

318

319

320 **Conclusion**

321 Assessment of fatty infiltration (FI) in rotator cuff muscles is important for predicting
322 shoulder conditions. Since 1994, the Goutallier score has been helping surgeons by using 2-
323 dimensional CT-scan slices. However, this 2D grading is associated with suboptimal
324 interobserver agreement. In this paper, we proposed three CT-based measurements for a
325 three-dimensional quantitative assessment of fatty infiltration (3DFI), muscle mass (3DMM),
326 and muscle loss (3DML). These new measures seem to provide a more consistent assessment

327 that still correlates well with Goutallier's principles. As 3DML measurements incorporate
328 atrophy and fatty infiltration, they have the potential to become a very reliable index for
329 assessing shoulder muscle function. Future algorithms capable of automatically calculating
330 the 3DML of the rotator cuff could be of great help in the decision process for rotator cuff
331 repair and the choice of anatomic or reverse shoulder arthroplasty.

332

333

334

335 **References**

- 336 1. Aubrey J, Esfandiari N, Baracos VE, Buteau FA, Frenette J, Putman CT et al.
337 Measurement of skeletal muscle radiation attenuation and basis of its biological variation.
338 *Acta Physiol (Oxf)* 2014;210:489-497. 10.1111/apha.12224
- 339 2. Beeler S, Ek ET, Gerber C. A comparative analysis of fatty infiltration and muscle
340 atrophy in patients with chronic rotator cuff tears and suprascapular neuropathy. *J Shoulder*
341 *Elbow Surg* 2013;22:1537-1546. 10.1016/j.jse.2013.01.028
- 342 3. Conze PH, Brochard S, Burdin V, Sheehan FT, Pons C. Healthy versus pathological
343 learning transferability in shoulder muscle MRI segmentation using deep convolutional
344 encoder-decoders. *Comput Med Imaging Graph* 2020;83:101733.
345 10.1016/j.compmedimag.2020.101733
- 346 4. Dekker TJ, Steele JR, Vinson EV, Garrigues GE. Current peri-operative imaging
347 concepts surrounding shoulder arthroplasty. *Skeletal Radiol* 2019;48:1485-1497.
348 10.1007/s00256-019-03183-3
- 349 5. Fuchs B, Weishaupt D, Zanetti M, Hodler J, Gerber C. Fatty degeneration of the
350 muscles of the rotator cuff: assessment by computed tomography versus magnetic resonance
351 imaging. *J Shoulder Elbow Surg* 1999;8:599-605.
- 352 6. Gerber C, Fuchs B, Hodler J. The results of repair of massive tears of the rotator cuff.
353 *J Bone Joint Surg Am* 2000;82:505-515.
- 354 7. Gerber C, Meyer DC, Schneeberger AG, Hoppeler H, von Rechenberg B. Effect of
355 tendon release and delayed repair on the structure of the muscles of the rotator cuff: an
356 experimental study in sheep. *J Bone Joint Surg Am* 2004;86:1973-1982. 10.2106/00004623-
357 200409000-00016
- 358 8. Gladstone JN, Bishop JY, Lo IK, Flatow EL. Fatty infiltration and atrophy of the
359 rotator cuff do not improve after rotator cuff repair and correlate with poor functional
360 outcome. *Am J Sports Med* 2007;35:719-728. 10.1177/0363546506297539

- 361 9. Goutallier D, Postel JM, Bernageau J, Lavau L, Voisin MC. Fatty muscle degeneration
362 in cuff ruptures. Pre- and postoperative evaluation by CT scan. *Clin Orthop Relat Res*
363 1994;78-83.
- 364 10. Hamada K, Fukuda H, Mikasa M, Kobayashi Y. Roentgenographic findings in
365 massive rotator cuff tears. A long-term observation. *Clin Orthop Relat Res* 1990:92-96.
- 366 11. Hashimoto T, Nobuhara K, Hamada T. Pathologic evidence of degeneration as a
367 primary cause of rotator cuff tear. *Clin Orthop Relat Res* 2003:111-120.
368 10.1097/01.blo.0000092974.12414.22
- 369 12. Holzbaur KR, Delp SL, Gold GE, Murray WM. Moment-generating capacity of upper
370 limb muscles in healthy adults. *J Biomech* 2007;40:2442-2449.
371 10.1016/j.jbiomech.2006.11.013
- 372 13. Holzbaur KR, Murray WM, Gold GE, Delp SL. Upper limb muscle volumes in adult
373 subjects. *J Biomech* 2007;40:742-749. 10.1016/j.jbiomech.2006.11.011
- 374 14. Jensen AR, Taylor AJ, Sanchez-Sotelo J. Factors Influencing the Reparability and
375 Healing Rates of Rotator Cuff Tears. *Curr Rev Musculoskelet Med* 2020. 10.1007/s12178-
376 020-09660-w
- 377 15. Jo CH, Shin JS. Changes in appearance of fatty infiltration and muscle atrophy of
378 rotator cuff muscles on magnetic resonance imaging after rotator cuff repair: establishing new
379 time-zero traits. *Arthroscopy* 2013;29:449-458. 10.1016/j.arthro.2012.10.006
- 380 16. Kalin PS, Crawford RJ, Marcon M, Manoliu A, Bouaicha S, Fischer MA et al.
381 Shoulder muscle volume and fat content in healthy adult volunteers: quantification with
382 DIXON MRI to determine the influence of demographics and handedness. *Skeletal Radiol*
383 2018;47:1393-1402. 10.1007/s00256-018-2945-1
- 384 17. Kenn W, Bohm D, Gohlke F, Hummer C, Kostler H, Hahn D. 2D SPLASH: a new
385 method to determine the fatty infiltration of the rotator cuff muscles. *Eur Radiol*
386 2004;14:2331-2336. 10.1007/s00330-004-2410-5
- 387 18. Khanna R, Saltzman MD, Elliott JM, Hoggarth MA, Marra GM, Omar I et al.
388 Development of 3D method to assess intramuscular spatial distribution of fat infiltration in
389 patients with rotator cuff tear: reliability and concurrent validity. *BMC Musculoskelet Disord*
390 2019;20:295. 10.1186/s12891-019-2631-z
- 391 19. Kuzel BR, Grindel S, Papandrea R, Ziegler D. Fatty infiltration and rotator cuff
392 atrophy. *J Am Acad Orthop Surg* 2013;21:613-623. 10.5435/JAAOS-21-10-613

- 393 20. Lambers Heerspink FO, Dorrestijn O. Editorial Commentary: Rotator Cuff Tear:
394 Know When Not to Operate So You Don't Make It Worse. *Arthroscopy* 2020;36:2091-2093.
395 10.1016/j.arthro.2020.06.019
- 396 21. Landis JR, Koch GG. The measurement of observer agreement for categorical data.
397 *Biometrics* 1977;33:159-174.
- 398 22. Lansdown DA, Morrison C, Zaid MB, Patel R, Zhang AL, Allen CR et al.
399 Preoperative IDEAL (Iterative Decomposition of Echoes of Asymmetrical Length) magnetic
400 resonance imaging rotator cuff muscle fat fractions are associated with rotator cuff repair
401 outcomes. *J Shoulder Elbow Surg* 2019;28:1936-1941. 10.1016/j.jse.2019.05.018
- 402 23. Lapner PL, Jiang L, Zhang T, Athwal GS. Rotator cuff fatty infiltration and atrophy
403 are associated with functional outcomes in anatomic shoulder arthroplasty. *Clin Orthop Relat*
404 *Res* 2015;473:674-682. 10.1007/s11999-014-3963-5
- 405 24. Maden-Wilkinson TM, McPhee JS, Rittweger J, Jones DA, Degens H. Thigh muscle
406 volume in relation to age, sex and femur volume. *Age (Dordr)* 2014;36:383-393.
407 10.1007/s11357-013-9571-6
- 408 25. Matsumoto F, Uthoff HK, Trudel G, Loehr JF. Delayed tendon reattachment does not
409 reverse atrophy and fat accumulation of the supraspinatus--an experimental study in rabbits. *J*
410 *Orthop Res* 2002;20:357-363. 10.1016/S0736-0266(01)00093-6
- 411 26. Matsumura N, Oguro S, Okuda S, Jinzaki M, Matsumoto M, Nakamura M et al.
412 Quantitative assessment of fatty infiltration and muscle volume of the rotator cuff muscles
413 using 3-dimensional 2-point Dixon magnetic resonance imaging. *J Shoulder Elbow Surg*
414 2017;26:e309-e318. 10.1016/j.jse.2017.03.019
- 415 27. Nakagaki K, Ozaki J, Tomita Y, Tamai S. Alterations in the supraspinatus muscle
416 belly with rotator cuff tearing: Evaluation with magnetic resonance imaging. *J Shoulder*
417 *Elbow Surg* 1994;3:88-93.
- 418 28. Nardo L, Karampinos DC, Lansdown DA, Carballido-Gamio J, Lee S, Maroldi R et al.
419 Quantitative assessment of fat infiltration in the rotator cuff muscles using water-fat MRI. *J*
420 *Magn Reson Imaging* 2014;39:1178-1185. 10.1002/jmri.24278
- 421 29. Nozaki T, Tasaki A, Horiuchi S, Osakabe C, Ohde S, Saida Y et al. Quantification of
422 Fatty Degeneration Within the Supraspinatus Muscle by Using a 2-Point Dixon Method on 3-
423 T MRI. *AJR Am J Roentgenol* 2015;205:116-122. 10.2214/AJR.14.13518
- 424 30. Oh JH, Kim SH, Choi JA, Kim Y, Oh CH. Reliability of the grading system for fatty
425 degeneration of rotator cuff muscles. *Clin Orthop Relat Res* 2010;468:1558-1564.
426 10.1007/s11999-009-0818-6

- 427 31. Pfirrmann CW, Schmid MR, Zanetti M, Jost B, Gerber C, Hodler J. Assessment of fat
428 content in supraspinatus muscle with proton MR spectroscopy in asymptomatic volunteers
429 and patients with supraspinatus tendon lesions. *Radiology* 2004;232:709-715.
430 10.1148/radiol.2323030442
- 431 32. Rueckert D, Schnabel JA. Model-Based and Data-Driven Strategies in Medical Image
432 Computing. In; 2019, p. arXiv:1909.10391.
- 433 33. Simovitch RW, Helmy N, Zumstein MA, Gerber C. Impact of fatty infiltration of the
434 teres minor muscle on the outcome of reverse total shoulder arthroplasty. *J Bone Joint Surg*
435 *Am* 2007;89:934-939. 10.2106/JBJS.F.01075
- 436 34. Slabaugh MA, Friel NA, Karas V, Romeo AA, Verma NN, Cole BJ. Interobserver and
437 intraobserver reliability of the Goutallier classification using magnetic resonance imaging:
438 proposal of a simplified classification system to increase reliability. *Am J Sports Med*
439 2012;40:1728-1734. 10.1177/0363546512452714
- 440 35. Spencer EE, Jr., Dunn WR, Wright RW, Wolf BR, Spindler KP, McCarty E et al.
441 Interobserver agreement in the classification of rotator cuff tears using magnetic resonance
442 imaging. *Am J Sports Med* 2008;36:99-103. 10.1177/0363546507307504
- 443 36. Tae SK, Oh JH, Kim SH, Chung SW, Yang JY, Back YW. Evaluation of fatty
444 degeneration of the supraspinatus muscle using a new measuring tool and its correlation
445 between multidetector computed tomography and magnetic resonance imaging. *Am J Sports*
446 *Med* 2011;39:599-606. 10.1177/0363546510384791
- 447 37. Terrier A, Ston J, Dewarrat A, Becce F, Farron A. A semi-automated quantitative CT
448 method for measuring rotator cuff muscle degeneration in shoulders with primary
449 osteoarthritis. *Orthop Traumatol Surg Res* 2017;103:151-157. 10.1016/j.otsr.2016.12.006
- 450 38. Thomazeau H, Rolland Y, Lucas C, Duval JM, Langlais F. Atrophy of the
451 supraspinatus belly. Assessment by MRI in 55 patients with rotator cuff pathology. *Acta*
452 *Orthop Scand* 1996;67:264-268.
- 453 39. Uthoff HK, Seki M, Backman DS, Trudel G, Himori K, Sano H. Tensile strength of
454 the supraspinatus after reimplantation into a bony trough: an experimental study in rabbits. *J*
455 *Shoulder Elbow Surg* 2002;11:504-509. 10.1067/mse.2002.126760
- 456 40. Vidt ME, Daly M, Miller ME, Davis CC, Marsh AP, Saul KR. Characterizing upper
457 limb muscle volume and strength in older adults: a comparison with young adults. *J Biomech*
458 2012;45:334-341. 10.1016/j.jbiomech.2011.10.007
- 459 41. Vidt ME, Santago AC, 2nd, Tuohy CJ, Poehling GG, Freehill MT, Kraft RA et al.
460 Assessments of Fatty Infiltration and Muscle Atrophy From a Single Magnetic Resonance

461 Image Slice Are Not Predictive of 3-Dimensional Measurements. *Arthroscopy* 2016;32:128-
462 139. 10.1016/j.arthro.2015.06.035

463 42. Williams MD, Ladermann A, Melis B, Barthelemy R, Walch G. Fatty infiltration of
464 the supraspinatus: a reliability study. *J Shoulder Elbow Surg* 2009;18:581-587.

465 10.1016/j.jse.2008.12.014

466 43. Young AA, Walch G, Pape G, Gohlke F, Favard L. Secondary rotator cuff dysfunction
467 following total shoulder arthroplasty for primary glenohumeral osteoarthritis: results of a
468 multicenter study with more than five years of follow-up. *J Bone Joint Surg Am* 2012;94:685-

469 693. 10.2106/JBJS.J.00727

470 44. Zanetti M, Gerber C, Hodler J. Quantitative assessment of the muscles of the rotator
471 cuff with magnetic resonance imaging. *Invest Radiol* 1998;33:163-170.

472

473

474 **Figure Legends**

475

476 Figure 1: Sagittal view of a right shoulder in a MRCT patient with severe fatty infiltration of
477 the supraspinatus and infraspinatus. Intra- and extra-muscular fat can be seen. This example
478 shows the difficulty to define precisely the difference between intra- and extra-muscular fat.

479

480 Figure 2: Example of a 42-year-old male from the healthy cohort.

481 Three-dimensional reconstruction and sagittal view of the left infraspinatus (red) and intra-
482 muscular fat (yellow).

483 V_{fibers} : muscle fiber volume

484 V_{imfat} : intra-muscular fat volume

485 V_{scapula} : scapular volume

486 NV_{fibers} : normalized volume of muscle fibers

487 Ref NV_{fibers} : reference value for *males* for the infraspinatus

488 3DMM: three-dimensional muscle mass

489 3DFI: three-dimensional quantitative calculation of fatty infiltration

490 3DML: three-dimensional muscle loss

491

492 Figure 3: Example of a 72-year-old female from the irreparable rotator cuff tear (IRCT)
493 cohort.

494 Three-dimensional reconstruction and sagittal view of the left infraspinatus (red) and intra-
495 muscular fat (yellow).

496 V_{fibers} : muscle fiber volume

497 V_{imfat} : intra-muscular fat volume

498 V_{scapula} : scapular volume

499 NV_{fibers} : normalized volume of muscle fibers

500 Ref NV_{fibers} : reference value for *females* for the infraspinatus

501 3DMM: three-dimensional muscle mass

502 3DFI: three-dimensional quantitative calculation of fatty infiltration

503 3DML: three-dimensional muscle loss

504

505

506

Table 1. Patient demographics

	Healthy Controls (46)	CTA (21)	IRCT (18)	OA (17)	All
Mean Age	36	77	71	69	56
± SD	± 16	± 8	± 8	± 8	± 22
Mean age Females	46	78	73	69	67
± SD	± 19	± 8	± 7	± 8	± 17
Mean sage Males	33	73	68	70	46
± SD	± 14	± 8	± 8	± 8	± 22
Left / Right	25 / 21	9 / 12	4 / 14	9 / 8	47 / 55
Females / Males	12/34	16/5	11/7	10/7	49/53

Table 1: Patient demographics

Table 2: Normalized muscles fiber volume (NV_{fibers}) for each condition.

		Healthy Controls		CTA		IRCT		OA	
Supraspinatus	M	0.65 ±0.1	0.67 ± 0.1	0.24 ±0.1	0.32 ± 0.1	0.27 ±0.1	0.31 ± 0.1	0.37 ±0.1	0.34 ± 0.1
	F		0.59 ± 0.1		0.21 ± 0.1		0.24 ± 0.1		0.39 ± 0.1
Subscapularis	M	1.89 ±0.3	1.98 ± 0.3	1.06 ±0.3	1.04 ± 0.4	1.03 ±0.2	1.05 ± 0.2	1.04 ±0.2	0.97 ± 0.2
	F		1.63 ± 0.2		1.07 ± 0.3		1.02 ± 0.3		1.09 ± 0.3
Infraspinatus	M	1.37 ±0.2	1.40 ± 0.2	0.65 ±0.3	0.73 ± 0.3	0.74 ±0.2	0.88 ± 0.1	0.92 ±0.2	0.90 ± 0.2
	F		1.29 ± 0.2		0.62 ± 0.3		0.66 ± 0.2		0.93 ± 0.2
Teres Minor	M	0.30 ±0.1	0.32 ± 0.1	0.21 ±0.1	0.25 ± 0.1	0.21 ±0.1	0.20 ± 0.1	0.19 ±0.1	0.20 ± 0.1
	F		0.26 ± 0.1		0.20 ± 0.1		0.21 ± 0.1		0.19 ± 0.1

Table 3: Inter-observer agreement for Goutallier classification (Fleiss' Kappa)

	Overall	
	Fleiss Kappa	95% CI
Supraspinatus	0.38	0.31 - 0.44
Subscapularis	0.27	0.22 – 0.33
Infraspinatus	0.42	0.35 – 0.48
Teres Minor	0.27	0.19 – 0.36

Table 4: Quantitative Three-Dimensional Fatty Infiltration (3D-FI). * represents values significantly different

	Healthy Controls		CTA		IRCT		OA		Kruskal-Wallis test
	2D Goutallier	3D-FI	2D Goutallier	3D-FI	2D Goutallier	3D-FI	2D Goutallier	3D-FI	
Supraspinatus	0.2 ±0.5	0.8% ±1.1%	2.3 ±0.9	15.9%* ±19% OA	2 ±0.7	11.7%* ±11% OA	1.4 ±0.7	4.6%* ±4% CTA/MRCT	P<0.02
Subscapularis	0 ±0	0.7% ±1.0%	1.2 ±0.6	8.9% ±10%	1.1 ±1.1	7.5% ±10%	0.4 ±0.5	3.9% ±3%	
Infraspinatus	0.2 ±0.4	0.6% ±0.9%	2.9 ±1.2	21%* ±19% OA	2.2 ±1.3	9.9% ±13%	1.2 ±0.8	3.3%* ±3% CTA	P<0.001
Teres Minor	0 ±0.1	0.7% ±2.0%	1.4 ±1.4	9% ±22%	0.9 ±1.1	4.4% ±10%	0.5 ±1	2.4% ±4%	

Table 5: Three-dimensional muscle loss (3D-ML) * represents values significantly different

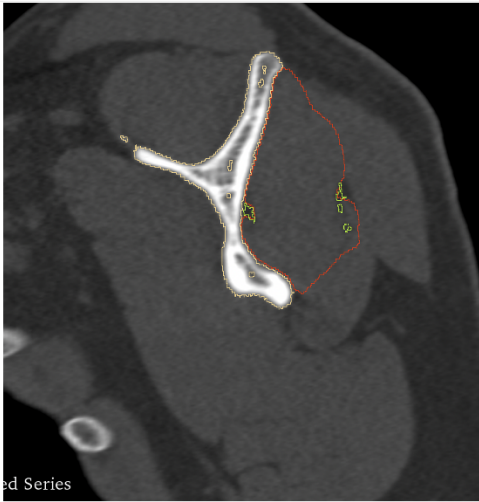
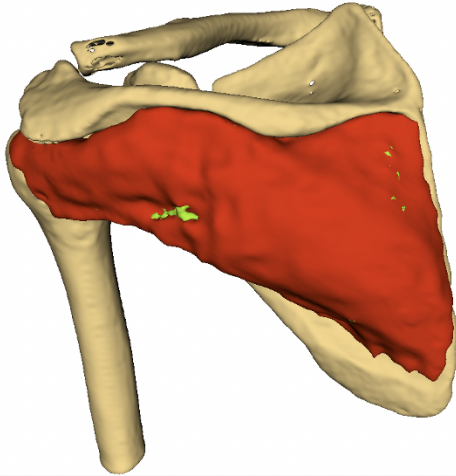
	Healthy Controls		CTA		IRCT		OA		ANOVA
	2D Goutallier	3D-ML	2D Goutallier	3D-ML	2D Goutallier	3D-ML	2D Goutallier	3D-ML	
Supraspinatus	0.2 ±0.5	0%	2.3 ±0.9	61%* ±13% OA	2 ±0.7	56%* ±16% OA	1.4 ±0.7	39%* ±14% CTA/MRCT	P<0.001
Subscapularis	0 ±0	0%	1.2 ±0.6	37% ±21%	1.1 ±1.1	41% ±14%	0.4 ±0.5	40% ±17%	
Infraspinatus	0.2 ±0.4	0%	2.9 ±1.2	51%* ±22% OA	2.2 ±1.3	44% ±16%	1.2 ±0.8	30%* ±15% CTA	P<0.005
Teres Minor	0 ±0.1	0%	1.4 ±1.4	22% ±36%	0.9 ±1.1	25% ±33%	0.5 ±1	30% ±44%	

Table 6: Correlation between the consensus Goutallier score and the quantitative 3D analysis of fatty infiltration (3D-FI) and muscle loss (3D ML)

	Goutallier	0	1	2	3	4	<i>rho</i>	<i>p-value</i>
Supraspinatus	<i>n</i>	38	24	30	7	3		
	3D-FI (%)	0.7 ± 1.2	2.2 ± 2.7	11.2 ± 10.2	25.3 ± 27	24.2 ± 13.9	0.79	<0.0001
	3D ML (%)	0.7 ± 0.5	25.6 ± 22.8	53.1 ± 15.2	72.7 ± 10.4	74.8 ± 4.0	0.87	<0.0001
Subscapularis	<i>n</i>	65	25	9	3	0		-
	3D-FI (%)	1.2 ± 1.6	6.3 ± 7.3	13.7 ± 8.7	22.2 ± 14.1	N/A	0.69	<0.0001
	3D ML (%)	10 ± 16.9	37.6 ± 18.5	50.2 ± 17.5	58.4 ± 12.2	N/A	0.69	<0.0001
Infraspinatus	<i>n</i>	43	26	9	12	12		-
	3D-FI (%)	0.6 ± 1.0	1.9 ± 2.2	7.5 ± 7.0	18.0 ± 14.1	29.7 ± 20.0	0.83	<0.0001
	3D ML (%)	2.3 ± 7.0	20.3 ± 18.6	36.5 ± 11.4	55.9 ± 10.5	62.6 ± 12.5	0.85	<0.0001
Teres Minor	<i>n</i>	71	20	4	2	5		-
	3D-FI (%)	0.8 ± 1.8	1.0 ± 1.3	17.4 ± 15.3	21.0 ± 10.1	31.7 ± 36.8	0.45	<0.0001
	3D ML (%)	5.3 ± 24.3	17.6 ± 25.3	50 ± 21.3	31 ± 21.2	84.2 ± 19.5	0.46	<0.0001
All muscles	<i>n</i>	217	95	52	24	20		
	3D-FI (%)	0.9 ± 1.5	2.9 ± 4.6	11.4 ± 9.9	20.7 ± 17.6	29.3 ± 23.4	0.71	<0.0001

	3D ML (%)	5.3 ± 17.4	25.6 ± 22.3	49.5 ± 16.3	59.7 ± 13.9	70.2 ± 16.3	0.74	<0.0001
--	------------------	-------------------	--------------------	--------------------	--------------------	--------------------	------	---------





Goutallier = 0

$$V_{\text{fibers}} = 175.98 \text{ cm}^3$$

$$V_{\text{imfat}} = 1.66 \text{ cm}^3$$

$$V_{\text{scapula}} = 111.67 \text{ cm}^3$$

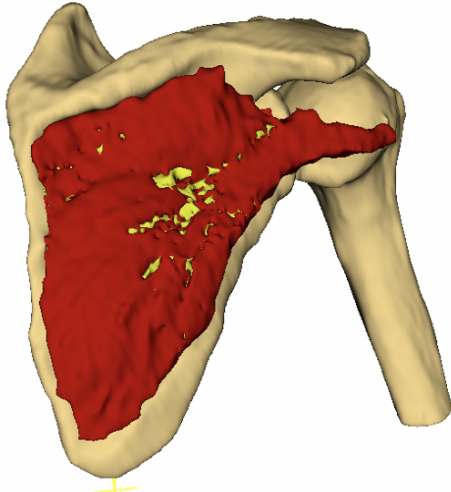
$$NV_{\text{fibers}} = \frac{V_{\text{fibers}}}{V_{\text{scapula}}} = 1.58$$

$$\text{Ref } NV_{\text{fibers}} = 1.40$$

$$3\text{DMM} = \frac{NV_{\text{fibers}}}{\text{Ref } NV_{\text{fibers}}} = 100\%$$

$$3\text{DFI} = \frac{V_{\text{imfat}}}{V_{\text{fibers}} + V_{\text{imfat}}} = 0.93\%$$

$$3\text{DML} = 100 - 3\text{DMM} = 0\%$$



Goutallier = 4

$$V_{\text{fibers}} = 45.72 \text{ cm}^3$$

$$V_{\text{imfat}} = 6.60 \text{ cm}^3$$

$$V_{\text{scapula}} = 87.51 \text{ cm}^3$$

$$NV_{\text{fibers}} = \frac{V_{\text{fibers}}}{V_{\text{scapula}}} = 0.52$$

$$\text{Ref } NV_{\text{fibers}} = 1.29$$

$$3\text{DMM} = \frac{NV_{\text{fibers}}}{\text{Ref } NV_{\text{fibers}}} = 41\%$$

$$3\text{DFI} = \frac{V_{\text{imfat}}}{V_{\text{fibers}} + V_{\text{imfat}}} = 12.61\%$$

$$3\text{DML} = 100 - 3\text{DMM} = 59\%$$